
This copy is for your personal, non-commercial use only.

If you wish to distribute this article to others, you can order high-quality copies for your colleagues, clients, or customers by [clicking here](#).

Permission to republish or repurpose articles or portions of articles can be obtained by following the guidelines [here](#).

The following resources related to this article are available online at www.sciencemag.org (this information is current as of May 6, 2011):

Updated information and services, including high-resolution figures, can be found in the online version of this article at:

<http://www.sciencemag.org/content/332/6030/708.full.html>

Supporting Online Material can be found at:

<http://www.sciencemag.org/content/suppl/2011/03/28/science.1202238.DC1.html>

This article **cites 25 articles**, 2 of which can be accessed free:

<http://www.sciencemag.org/content/332/6030/708.full.html#ref-list-1>

This article has been **cited by** 2 articles hosted by HighWire Press; see:

<http://www.sciencemag.org/content/332/6030/708.full.html#related-urls>

This article appears in the following **subject collections**:

Planetary Science

http://www.sciencemag.org/cgi/collection/planet_sci

M. Norell, R. Papendieck, O. Rauhut, M. Sander, K. Seymour, B. Shaffer, D. Unwin, X. Xu, and Z. Zhou granted specimen access. The project was supported by NSF grant EAR 0551024 to R.M. and Durrell Funds of the Department of Geology, University of California Davis, an M. A. Fritz Award of Royal Ontario Museum, a doctoral stipend of German Academic Exchange Service,

and a postdoctoral fellowship of German Research Foundation to L.S.

Supporting Online Material

www.sciencemag.org/cgi/content/full/science.1200043/DC1
Materials and Methods
SOM Text

Figs. S1 and S2
Tables S1 to S5
References

5 November 2010; accepted 16 February 2011
Published online 14 April 2011;
10.1126/science.1200043

Saturn's Curiously Corrugated C Ring

M. M. Hedman,^{1*} J. A. Burns,^{1,2} M. W. Evans,¹ M. S. Tiscareno,¹ C. C. Porco³

In August 2009 the Sun illuminated Saturn's rings from almost exactly edge-on, revealing a subtle corrugation that extends across the entire C ring. This corrugation's amplitude is 2 to 20 meters and its wavelength is 30 to 80 kilometers. Radial trends in the corrugation's wavelength indicate that this structure—like a similar corrugation previously identified in the D ring—results from differential nodal regression within a ring that became tilted relative to Saturn's equator plane in 1983. We suggest that this initial tilt arose because interplanetary debris struck the rings. The corrugation's radial extent implies that the impacting material was a dispersed cloud of debris instead of a single object, and the corrugation's amplitude indicates that the debris' total mass was $\sim 10^{11}$ to 10^{13} kilograms.

The Cassini spacecraft obtained numerous images of Saturn's rings within a few months of Saturn's equinox in August 2009, when the Sun illuminated the rings from almost exactly edge-on. Many of these observations were designed to investigate ring features that would be highlighted by this unusual lighting geometry, such as shadows cast by embedded moonlets or inclined ringlets. Among

the most surprising structures revealed by these images was a series of regularly spaced bright and dark bands extending throughout the entire C ring (Fig. 1). Because this periodic banding was not seen in earlier Cassini images, it cannot be ascribed to simple variations in the ring's density or optical depth. Instead, these bands appear to be caused by a vertical corrugation extending across the entire C ring. Broad-scale corrugations have previously been identified in Saturn's D ring (1) and Jupiter's main ring (2); both these structures appear to have formed within the last few decades when the relevant ring suddenly became tilted relative to its planet's equatorial plane (1, 3). The C-ring corrugation seems to have been similarly generated, and

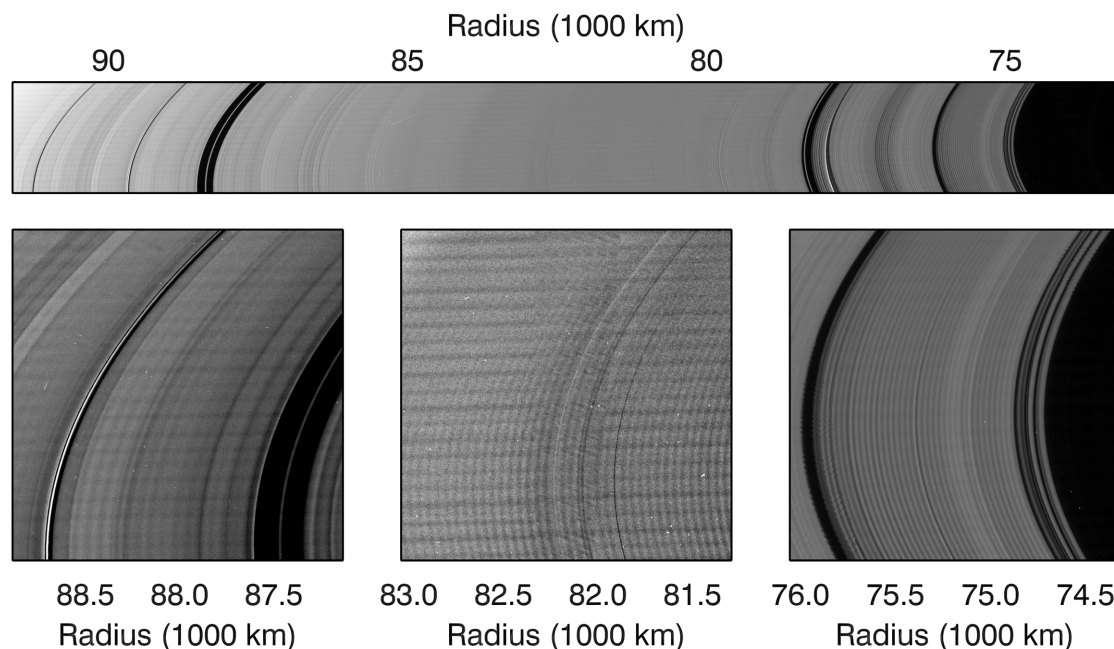
indeed it was probably created by the same ring-tilting event that produced the D-ring's corrugation.

The amplitudes and wavelengths of the C-ring's periodic brightness variations have been measured using Fourier analyses of selected images (SOM text 1). The amplitudes of the observed brightness variations change with viewing and illumination geometries as expected for a vertically corrugated ring (SOM text 2). The corrugation amplitudes derived with a simple photometric model range between 2 and 20 m throughout the C ring (Fig. 2A; SOM text 2 describes systematic uncertainties associated with these estimates), and are thus well below the few-hundred-meter amplitudes of the previously identified D-ring corrugations (1). Meanwhile, the corrugation wavenumber systematically decreases with increasing distance from Saturn throughout the entire C ring (Fig. 2B), suggesting that the observed corrugations are part of a single coherent structure. Extrapolating the observed trends interior to the C ring shows that the predicted wavenumber is close to the expected wavenumber of the previously observed, larger-amplitude D-ring corrugation. The latter has been interpreted as the result of differential nodal regression of an initially inclined ring (1), which suggests that the C-ring corrugations could have been produced by the same process (Fig. 3). Indeed, the radial trends seen in Fig. 2B are consistent with such a model.

¹Department of Astronomy, Cornell University, Ithaca, NY 14853, USA. ²Department of Mechanical Engineering, Cornell University, Ithaca, NY 14853, USA. ³CICLOPS—Space Science Institute, Boulder, CO 80301, USA.

*To whom correspondence should be addressed. E-mail: mmhedman@astro.cornell.edu

Fig. 1. Mosaic of images of Saturn's C ring obtained during Cassini's orbit 117, along with close-ups of selected radial regions showing the periodic bright and dark bands that extend across the entire C ring. The contrast has been adjusted in each close-up image to better show the periodic structure. Horizontal bands within these close-ups are camera artifacts (22).



A corrugation produced by differential nodal regression of an initially inclined ring should have a radial wavenumber given by [SOM text 3 and (1)]

$$k_z \approx \left| \frac{\partial \dot{\Omega}}{\partial r} \right| \delta t \quad (1)$$

where δt is the time that has elapsed since the ring was an inclined sheet, and $\dot{\Omega}$ is the local nodal regression rate. To first order, $\dot{\Omega}$ is determined by Saturn's quadrupole gravitational harmonic J_2 (4, 5), so Eq. 1 can be approximated as

$$k_z \approx \frac{21}{4} J_2 \sqrt{\frac{GM_S}{r^5}} \left(\frac{R_S}{r} \right)^2 \delta t \quad (2)$$

where G is the gravitational constant, M_S is Saturn's mass, r is the ring radius, and R_S is the assumed Saturn radius used to normalize J_2 . Thus, a corrugation produced by differential nodal regression should have $k_z \sim r^{-9/2}$. Including contributions from all Saturn's measured higher-order gravity harmonics (6) yields the solid curves in Fig. 2, B and C, which differ slightly from the trend calculated above and match the observed data to within 3%.

The largest deviations from this model include a quasi-periodic wavenumber modulation in the middle C ring and a cluster of low wavenumber values in the outermost C ring ($r > 90,000$ km, Fig. 2C). These residuals are correlated with the optical depth structure of the ring (compare Fig. 2, C and E) and can be ascribed to the C-ring's finite surface mass density σ . The ring's gravity modifies the local nodal regression rates, producing perturbations to the corrugation wavenumber:

$$\frac{\delta k_z}{k_z} = \frac{\pi G}{2v} \left(-\frac{\partial \sigma}{\partial r} + \frac{3\sigma}{r} \right) \delta t \quad (3)$$

where v is the vertical epicyclic frequency (SOM text 3). If we assume that the ring's optical depth τ is proportional to its surface mass density σ , then the largest negative residuals in the corrugation wavenumber should occur where the optical depth has the most positive slope and vice versa, as observed. Furthermore, the magnitude of the measured residuals would require that the middle C ring has $\sigma \sim 3$ to 6 g/cm² (SOM text 4), consistent with previous estimates (7, 8).

If we only consider regions where the predicted $\delta k_z/k_z$ caused by the ring's self-gravity is less than 0.2% (Fig. 2D and SOM text 5), the wavelength estimates are fully consistent with predicted trends based on current estimates of Saturn's gravity field (6). We may therefore use Eq. 1 to determine how long ago the C ring was a simple inclined sheet: Julian date (JD) 2445598 ± 40 , or day 263 ± 40 of 1983 (9). This is within a year of the inclined sheet epoch derived from the previously observed temporal variations in the D-ring's corrugation wavelength (1), and the difference between the two estimates may be attributed to the excess variance in the D-ring wavelength estimates derived from images taken in different viewing geometries (1). It is therefore reasonable to conclude that the corrugations in both the C and D rings were generated by the same ring-tilting event.

Saturn was near solar conjunction during the latter half of 1983 and thus could not be seen clearly from Earth. Archived images therefore cannot provide direct information about any event that might have caused the rings to become tilted relative to Saturn's gravitational equator. However, any acceptable scenario must be

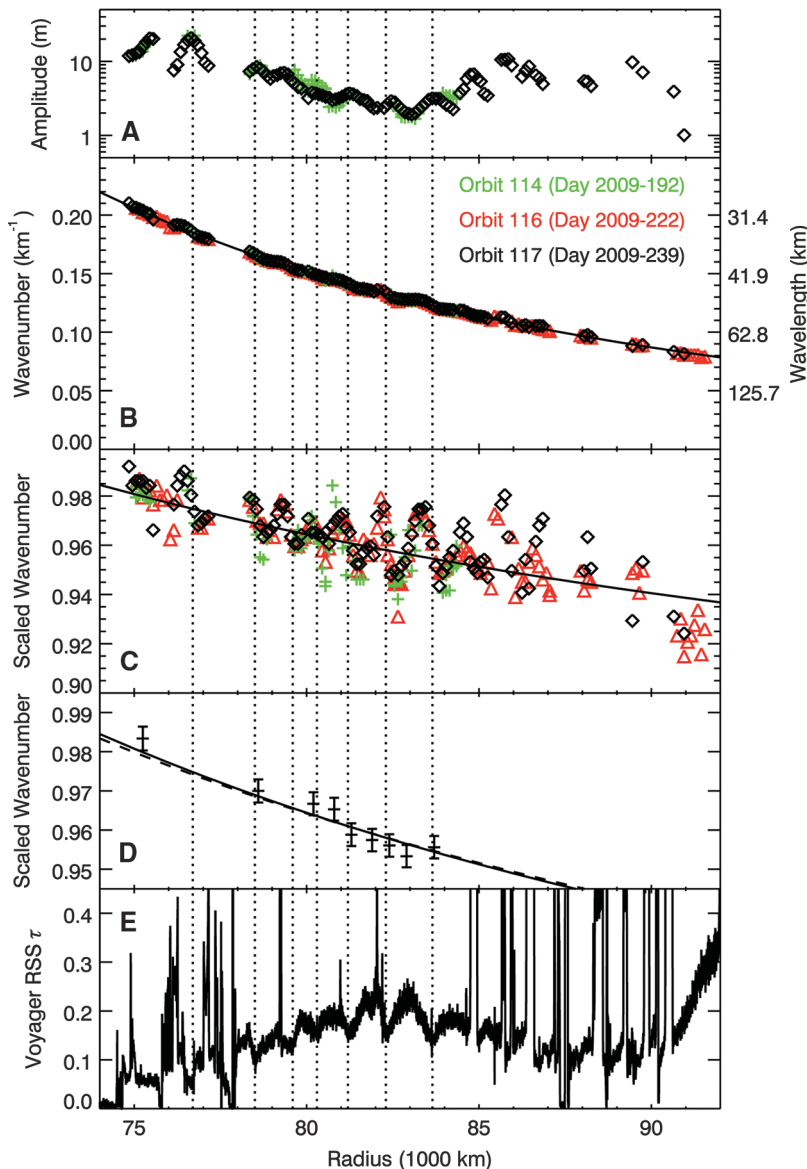
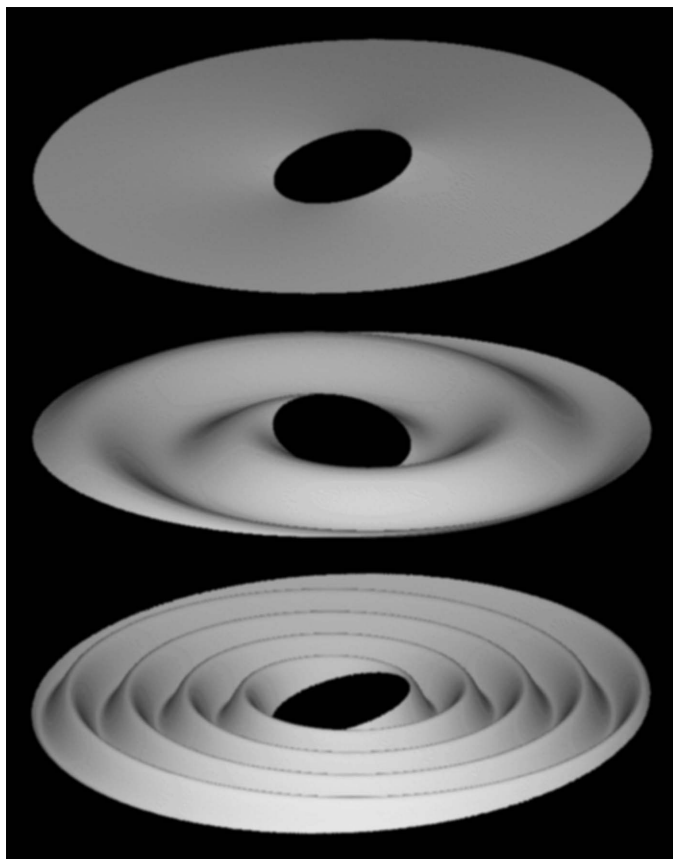


Fig. 2. Corrugation parameters versus radius in the rings (distance from Saturn's spin axis) derived from three observations taken on three different Cassini orbits around the time of Saturn's equinox (see SOM text 1 and 2 for analysis procedures): (A) Corrugation amplitude A_z , (B) corrugation wavenumber k_z , and (C) scaled corrugation wavenumber $k'_z = k_z/k_0 \times (r/r_0)^{9/2}$, where $k_0 = (2\pi/40)$ km⁻¹ $r_0 = 80,000$ km are constants chosen to normalize k'_z to approximately unity at equinox. In these plots, each data point is computed from a Fourier analysis of a 500-km-wide ring region, so adjacent data points from the same observation, which are separated by only 100 km, are not independent. No amplitudes are plotted for the Orbit 116 data because the extremely low Sun-opening angle during these observations complicates the photometry (see SOM text 2). (D) Estimates and uncertainties (1 standard deviation) of the rescaled corrugation wavenumber at JD 2455054 at locations in the ring where the finite mass of the ring can be neglected (SOM text 5). The solid curves in (B), (C), and (D) are the predicted wavenumber of a vertical corrugation produced by differential nodal regression of an inclined ring that existed at JD 2445598, assuming the standard model of Saturn's gravity field (6) with $J_n = 0$ for $n > 8$. In (D), the dashed curve shows a similar prediction, assuming $J_8 = 0$ instead of $J_8 = -0.00001$. (E) Normal optical depth profile of the C ring measured by the Voyager Radio Science Subsystem (obtained from the Planetary Data System rings node).

Fig. 3. Cartoon representation of how differential nodal regression produces a vertical corrugation from an initially inclined ring. The top image shows a simple inclined ring (the central planet is omitted for clarity), while the lower two images show the same ring at two later times, where the orbital evolution of the ring particles has sheared this inclined sheet into an increasingly tightly wound spiral corrugation.



able to produce a tilt across a wide swath of the ring in a short period of time compared to the local orbital precession periods (which range between 2 weeks and 1 month). Preliminary calculations suggest that Saturn's equator is unlikely to shift appropriately due to either external torques on Saturn or mass redistribution within the planet (SOM text 6). Furthermore, recent analyses of Galileo data indicate that Jupiter's rings became tilted around the time comet Shoemaker-Levy 9 struck the planet in 1994 (3). We therefore investigate scenarios in which the rings became tilted relative to Saturn's equator plane due to interplanetary debris impacting the rings in 1983.

The estimated corrugation amplitudes in the C ring (Fig. 2A) indicate that the entire C ring was initially tilted relative to Saturn's equator plane by an angle $\delta\theta$ between 2×10^{-8} and 3×10^{-7} radians. Assuming a ring surface mass density of $\sim 5 \text{ g/cm}^2$ (see above), the ring's angular momentum would need to reorient by $\delta L_r \sim 10^{23} \text{ kg m}^2/\text{s}$ to produce this tilt. Although a reasonably dense ($\sim 1 \text{ g/cm}^3$) 1-km-wide object traveling at typical impact speeds through the rings ($\sim 40 \text{ km/s}$, comparable to the escape speed from Saturn) would carry sufficient angular momentum to produce the required δL_r , it is unlikely that an intact comet or meteoroid could have produced a feature as radially extensive as the observed corrugation. A compact object $\sim 1 \text{ km}$ across passing through the C ring

would only interact with a small patch of the rings containing $<10^{-3}$ the mass of the impactor, so any debris from this collision would follow essentially the same trajectory as that of the pre-impact projectile. Thus, most of the incoming object's momentum would escape in the debris from the collision and not be imparted to the rings, and no large-scale tilt would be established. However, if the rings encountered a diffuse cloud of debris instead of a single solid object, then material would have rained down across a range of radii, producing a tilt that could ultimately form an extensive corrugation. The incoming debris would also interact with a much larger area of the rings and a much greater mass of ring material, so more of the momentum carried by the debris should remain in the ring instead of departing from the Saturn system. Such a scenario could even explain the differences in the corrugation amplitudes between the C and D rings. Assuming the momenta from the incoming particles are efficiently transferred to the rings (SOM text 7), the tilt induced by a given debris flux should be directly proportional to the ring particles' aggregate cross section and inversely proportional to their total mass. The larger amplitude of the D-ring corrugation could therefore arise simply because the submillimeter-wide particles in the D ring (1) have much higher surface-area-to-volume ratios than the centimeter-to-meter-sized C-ring particles (10).

The viability of this explanation for the ring's initial tilt can be evaluated by estimating the total debris mass required to produce the observed corrugations. For rings of modest optical depth like the C ring, the angular momentum delivered into the rings by a debris cloud of mass m_c can be expressed as

$$L_c = D_F \tau m_c v_c r \quad (4)$$

where v_c is the mean impact speed of the incoming material, r and τ are the orbital radius and normal optical depth of the ring, and D_F is a dimensionless parameter that depends on the longitudinal distribution of the impacting material. For a homogeneous debris cloud, $D_F \sim 0.1$ for a wide range of plausible approach trajectories and speeds (SOM text 7), and it could be higher if the cloud has substantial substructure. Assuming that D_F lies between 1 and 0.01, and further stipulating that $L_c \approx \delta L_r \sim 10^{23} \text{ kg m}^2/\text{s}$, $v_c \approx 40 \text{ km/s}$, and $\tau \sim 0.1$ (Fig. 2E), we find that the total mass of the debris cloud would need to be 10^{11} to 10^{13} kg in order to produce the observed C-ring corrugation.

Debris clouds with masses on the order of 10^{12} kg were produced during the break-up of Shoemaker-Levy 9 in 1992 (11, 12) and the major outburst of comet 17P/Holmes in 2007 (13). The rate at which Saturn would encounter such massive clouds is quite uncertain, but consider the specific scenario where a 1-km-wide comet nucleus was captured into orbit around Saturn and broke apart during a close periape passage (due to planetary tides or a collision with the rings), producing $\sim 10^{12} \text{ kg}$ of debris on bound orbits that crashed into the rings on a later periape (14). Although the rate at which captured cometary debris impacts Saturn has not yet been thoroughly investigated in numerical simulations, existing studies indicate that roughly 4% of the comets that impact Jupiter had previously passed close enough to the planet to be disrupted (15), the impact flux at Saturn is about 40% the flux at Jupiter (16, 17), and the fraction of impactors on bound orbits is about an order of magnitude less for Saturn than it is for Jupiter (18–20). Together, these results indicate that Saturn should encounter debris clouds derived from comets disrupted by previous planetary encounters at a rate that is roughly 0.2% of Jupiter's impact rate. The 2009 detection of a fresh impact scar at Jupiter suggests that 1-km-wide objects may strike Jupiter as often as once a decade (21). In this case, the clouds of orbiting debris created by the disruption of a 1-km-wide comet should rain down on Saturn's rings once every 5000 to 10,000 years. The probability that debris from a previously disrupted comet would hit Saturn's rings in the last 30 years would then be between roughly 1% and 0.1%, which is not very small. Such scenarios therefore provide a reasonable explanation for the origin of the observed corrugation in Saturn's C ring.

References and Notes

1. M. M. Hedman *et al.*, *Icarus* **188**, 89 (2007).
2. M. E. Ockert-Bell *et al.*, *Icarus* **138**, 188 (1999).
3. M. R. Showalter, M. M. Hedman, J. A. Burns, *Science* **332**, 711 (2011).
4. C. D. Murray, S. F. Dermott, *Solar System Dynamics* (Cambridge Univ. Press, Cambridge, 1999).
5. For Saturn's C ring, higher-order gravity harmonics, mainly J_4 (6), only contribute a total of <10% to the nodal regression rate and 10 to 15% to the gradient of the nodal regression rate.
6. R. A. Jacobson *et al.*, *Astron. J.* **132**, 2520 (2006).
7. H. A. Zebker, E. A. Marouf, G. L. Tyler, *Icarus* **64**, 531 (1985).
8. P. A. Rosen, G. L. Tyler, E. A. Marouf, J. J. Lissauer, *Icarus* **93**, 25 (1991).
9. The error estimate includes ± 10 days of statistical error, ± 13 days uncertainty from the published estimate of J_6 (6), ± 13 days from allowing J_8 to range between 0 and -0.00001 , and ± 5 days that depends on whether the wavenumbers are corrected for the ring's predicted mass. Additional uncertainty could be introduced if J_{10} and higher-order terms in Saturn's gravity field are sufficiently large.
10. J. N. Cuzzi *et al.*, in *Saturn From Cassini-Huygens*, M. K. Dougherty, L. W. Esposito, S. M. Krimigis, Eds. (Springer, New York, 2009), pp. 459–509.
11. J. V. Scotti, H. J. Melosh, *Nature* **365**, 733 (1993).
12. E. Asphaug, W. Benz, *Icarus* **121**, 225 (1996).
13. M. Montalto, A. Riffeser, U. Hopp, S. Wilke, G. Carraro, *Astron. Astrophys.* **479**, L45 (2008).
14. Scenarios in which the debris from the disrupted comet hits the rings before it can leave the inner Saturn system are explored in SOM text 8 and are found to be less probable.
15. D. M. Kary, L. Dones, *Icarus* **121**, 207 (1996).
16. H. F. Levison, M. J. Duncan, *Icarus* **127**, 13 (1997).
17. K. Zahnle, P. Schenk, H. Levison, L. Dones, *Icarus* **163**, 263 (2003).
18. H. F. Levison, M. J. Duncan, K. Zahnle, M. Holman, L. Dones, *Icarus* **143**, 415 (2000).
19. S. Charnoz, A. Morbidelli, L. Dones, J. Salmon, *Icarus* **199**, 413 (2009).
20. This rate may be conservative because none of the referenced simulations include Saturn's rings, which could not only disrupt incoming comets but also withdraw some momentum from the debris, increasing its chances of being captured into orbit around Saturn.
21. A. Sánchez-Lavega *et al.*, *Astrophys. J.* **715**, L155 (2010).
22. C. C. Porco *et al.*, *Space Sci. Rev.* **115**, 363 (2004).

Acknowledgments: We acknowledge the support of the Imaging Science Subsystem team and the Cassini Project, as well as NASA's Planetary Geology and Geophysics, and Cassini Data Analysis programs. We also thank M. R. Showalter, P. D. Nicholson, S. Charnoz, L. Dones, and D. P. Hamilton for useful conversations.

Supporting Online Material

www.sciencemag.org/cgi/content/full/science.1202238/DC1
SOM Text
Figs. S1 to S5
Tables S1 to S3
References

27 December 2010; accepted 16 March 2011

Published online 31 March 2011;

10.1126/science.1202238

The Impact of Comet Shoemaker-Levy 9 Sends Ripples Through the Rings of Jupiter

Mark R. Showalter,^{1*} Matthew M. Hedman,² Joseph A. Burns²

Jupiter's main ring shows vertical corrugations reminiscent of those recently detected in the rings of Saturn. The Galileo spacecraft imaged a pair of superimposed ripple patterns in 1996 and again in 2000. These patterns behave as two independent spirals, each winding up at a rate defined by Jupiter's gravity field. The dominant pattern originated between July and October 1994, when the entire ring was tilted by about 2 kilometers. We associate this with the Shoemaker-Levy 9 impacts of July 1994. New Horizons images still show this pattern 13 years later and suggest that subsequent events may also have tilted the ring. Impacts by comets or their dust streams are regular occurrences in planetary rings, altering them in ways that remain detectable decades later.

On 9 November 1996, the Galileo spacecraft imaged a systematic, unexplained pattern of brightness variations in Jupiter's main ring, suggesting vertical ripples in the ring's surface (1). More recently, Cassini images have revealed a similar pattern in Saturn's rings. The latter pattern arose from an initially inclined ring, which was slowly twisted into a spiral by Saturn's gravity (2, 3). A closer analysis of Galileo data now confirms that the patterns in the rings of Jupiter and Saturn obey identical kinematics, except that Jupiter's ring contains two ripple patterns, not one.

Galileo viewed the rings from nearly edge-on, with opening angle $B = 0.48^\circ$ (Fig. 1 and table S1). The intensity I of an optically thin ring is proportional to the amount of material along the

line of sight, so it varies as $\sin(B)^{-1}$. For the jovian ring, optical depth $\tau < 10^{-5}$ (4, 5), so this dependence applies. In this limit, the Sun's opening angle plays no role, because every particle is illuminated equally.

A nonzero surface slope modifies the effective local opening angle, naturally leading to variations in I (6).

$$I \propto 1/\sin(B)[1 - \sin(\theta)/\sin(B)Z'(R,\theta)] \quad (1)$$

Here, $Z(R,\theta)$ describes the local height of the ring above the equatorial plane in polar coordinates (R,θ) . The radial component of the local slope is $Z'(R,\theta) \equiv \partial Z/\partial R$; we neglect the slope's much smaller tangential component (6, 7). Longitudes are measured from the ansa line passing through the ring's tip, where a radial vector is perpendicular to the line of sight.

The dependence of I on $\sin(\theta)$ naturally predicts the reversals of contrast observed in the Galileo image. We have applied Eq. 1 to derive

the function $Z'(R)$ at $\theta = 0$ (Fig. 1C). Slopes approach 3% or $\sim 1.5^\circ$. However, unlike the pattern in Saturn's rings (2, 3), this one is not a pure sinusoid; a Fourier transform shows two distinct peaks (Fig. 2A). In a least-squares modeling of $Z'(R)$, two sinusoids successfully account for the location of nearly every peak and trough. Matches to the amplitudes are imperfect, however, suggesting that the ring slope may be modulated by other factors that we have not yet considered. The dominant pattern has a wavelength $\lambda_{\text{long}} = 1920 \pm 150$ km and a vertical amplitude $Z_{\text{long}} = 2.4 \pm 0.7$ km; the shorter-wavelength pattern has $\lambda_{\text{short}} = 630 \pm 20$ km and $Z_{\text{short}} = 0.6 \pm 0.2$ km.

If these sinusoidally varying slopes are analogous to the corrugations observed at Saturn (2, 3), then they arose from an initially tilted ring that slowly twisted into a spiral pattern as a result of differential nodal regression. The wavelength of these patterns depends only on the local gravitational field and the amount of time T that has elapsed since the ring became tilted (2, 3). Near the middle of the main jovian ring, the predicted wavelength is

$$\lambda = \sim 4200 \text{ km}/(T/\text{years}) \quad (2)$$

The numerical factor is derived from Jupiter's gravitational harmonics (8). It varies by $\sim 15\%$ within the radial limits considered but for practical purposes can be treated as a constant when modeling individual profiles (6).

Compared with Saturn's ~ 30 -km periodicity, the longer wavelengths at Jupiter would imply much more recent features. For the long-wavelength pattern, $T = 800 \pm 60$ days, indicating that a ring-tilting event occurred between 1 July and 1 November 1994. The shorter wavelength corresponds to $T = 2430 \pm 80$ days, meaning that the feature originated between early January and early June 1990; the midpoint is 19 March.

Two Galileo images from 21 June 2000 confirm that this pattern is evolving in the predicted

¹SETI Institute, 189 Bernardo Avenue, Mountain View, CA 94043, USA. ²Department of Astronomy, Cornell University, Ithaca NY 14853, USA.

*To whom correspondence should be addressed. E-mail: mshowalter@seti.org